

Snow Particle Size Spectra in Lake Effect Snows

ROSCOE R. BRAHAM, JR.

University of Chicago, Chicago, Illinois

(Manuscript received 29 April 1989, in final form 8 September 1989)

ABSTRACT

In situ snow particle size spectra measured by Particle Measuring Systems probes near the downwind shore of Lake Michigan during lake-effect snow storms are presented and discussed. Ice water contents ranged from 0.002 to 0.264 g m⁻³. Concentrations of sizes larger than 1 mm were generally exponentially distributed; however, concentrations of smaller particles usually were greater than suggested by the exponential fitted to concentrations of sizes larger than 1 mm. Exponential distribution parameters (N_0 and λ) are consistent with previously reported values. There is evidence for particle aggregation at -25°C .

1. Introduction

In contrast to the situation for raindrops, relatively few in situ measurements of snow particle size spectra have been published. The purpose of this brief article is to present several examples of snow particle size spectra measured in situ with Particle Measuring Systems (PMS) probes. These data were obtained during the University of Chicago study of lake-effect snow storms over Lake Michigan. This article is restricted to measurements made within 500 m of the lake surface, near the downwind shore during well-developed lake-effect snow events. A more general article on snow in lake-effect storms over Lake Michigan is in preparation.

Prior to the development of PMS probes (Knollenberg 1970, 1976, 1981), it was virtually impossible to obtain in situ snow particle spectra. Individual ice crystals can be collected on small slides exposed from aircraft, but snowflakes are too fragile to be collected in that manner. Efforts to decelerate snow particles prior to slide collection were successful only for the smallest particles. Many of the snow particle size spectra in the literature were derived from size spectra of particles collected on a horizontal surface [e.g., Gunn and Marshall (1958); Rogers (1974)]. From knowledge of the area of the collecting surface and duration of the collection, and making use of an assumed relation between particle sizes and fall speeds, one can derive spatial (free-space) distributions. To avoid the uncertainties of an assumed fall-speed relation, Ohtake (1965, 1968) preferred to deal with horizontal surface spectra.

The horizontal surface technique has several inherent difficulties. Particle fall speeds vary with size, shape and bulk density, making it necessary to use different fall speed relations appropriate to different particle types. Difficulties arise from wind effects that can cause biases in the sizes of particles collected. In addition, it is difficult for experimenters to handle small particles, and to cope with the large numbers of particles required for good sampling statistics.

Marshall and Gunn (1952) noted that for ice and snow particles small enough to be in the Rayleigh scattering region, the radar cross section would be the same as that of a sphere of ice having the same mass (Smith 1984). This led to a series of studies in which snow particles collected on surfaces at the ground were melted and the masses of the melted particles determined. Then by using a fall speed relation for the original unmelted particles, the derived spatial distributions were expressed in terms of melted particle sizes [e.g., see Gunn and Marshall (1958); Battan (1973); Smith (1984); and Sekhon and Srivastava (1970)]. This procedure completely bypassed the complex issues of snowflake size, shape and bulk density, while providing reflectivity relationships needed for interpreting radar signals from snow. Unfortunately it also distracted attention from the issue of unmelted snowflake size spectra needed for theoretical and modeling studies of snow development.

Passarelli (1978a,b), Passarelli et al. (1976), Houze et al. (1979), Lo and Passarelli (1982), and Gordon and Marwitz (1984), have reported in situ spectra of snow particles in deep cyclonic storm systems. With the exception of Gordon and Marwitz, these authors use data from PMS one-dimensional probes having upper-size limits of about 4.5 mm. The data reported by Gordon and Marwitz were obtained by combining data from three different PMS probes (both one- and

Corresponding author address: Prof. Roscoe R. Braham, Jr., The University of Chicago, Dept. of the Geophysical Sciences, 5734 South Ellis Avenue, Chicago, IL 60637.

two-dimensional) for sizes below 4 mm. All these authors reported spectra from several levels and emphasized snow growth processes. In contrast to these other studies, data reported here were obtained near the surface, well-removed from snow growth regions. These data were obtained by combining information from three different PMS probes covering sizes to over 6 mm diameter.

2. Instrumentation and data

Project Lakesnow operations were conducted from Muskegon, Michigan. All data reported here were obtained during December 1983 and January 1984 from aircraft flights into lake-effect snow storms over Lake Michigan. These storms are characterized by a broken layer of stratocumulus clouds having ragged bases, typically 0.3 to 0.5 km above the lake, and rather smooth tops, 1.0 to 1.5 km above the lake. Measured temperatures 100 m above the lake often are 15°–20°C colder than the unfrozen lake surface, resulting in strongly superadiabatic surface layers. Strong fluxes of heat and moisture from the surface layer produce vigorous convective stirring within and below the clouds. Cloud updrafts of 1–2 m s⁻¹, averaged over scales of 500–1000 m, contain 100-m sized cores up to 4–5 m s⁻¹. Significant downdrafts (1–2 m s⁻¹) are observed inside, between, and below the clouds. Cloud drop concentrations in cloud cores are 700–1000 cm⁻³ (measured by the FSSP). Peak values of cloud liquid are about 0.2 to 0.3 g m⁻³ in updraft cores (measured by the JW probe). In the upper third of the boundary layer (i.e., in the entrainment zone) snow is restricted to cloudy air. In the lower half of the boundary layer snow is found over 80–90 percent of the area. Snow growth obviously is a maximum in the upward-moving air parcels. Convective stirring results in considerable

TABLE 1. Size intervals used in evaluating snow data from the PMS 200Y probe. Based upon Knollenberg (1975, Fig. 17) for a probe with a nominal array spacing of 200 micrometers. Values are given in millimeters.

Interval number	Lower size limit	Upper size limit
1	0.250	0.600
2	0.600	0.944
3	0.944	1.288
4	1.288	1.632
5	1.632	1.975
6	1.975	2.319
7	2.319	2.663
8	2.663	3.007
9	3.007	3.351
10	3.351	3.695
11	3.695	4.038
12	4.038	4.382
13	4.382	4.726
14	4.726	5.070
15	5.070	5.242

TABLE 2. Characteristics of probes used in this study. Nominal values unless specified otherwise.

Probe	Resolution micrometers	Max size measured micrometers	Sample vol. liters per min.
200Y	200	4500 (5240) ^a	3500 ^b
2D-C	50	2000 (1754) ^c	(50–500) ^d
2D-P	200	7100 (6230) ^c	(1000–7000) ^d

^a After Knollenberg (1975) adjustment.

^b For 4-mm diam particles; decreases for smaller particles.

^c After clocking error adjustment.

^d Sample volume depends on probe activity. Values given show range of sample volumes for samples used in this paper.

recycling of snow particles between updrafts and downdrafts. Downdrafts below 500 m often are sub-saturated with respect to ice, resulting in evaporation of snow particles.

In situ size spectra were obtained from PMS 200Y, 2D-C, and 2D-P probes mounted on NCAR King Air N312D. [For a description of these probes see Knollenberg (1970, 1976, 1981).] Data from the 200Y probes were adjusted to reflect the reduced sizing capability of these probes for ice and snow particles. Knollenberg (1975, 1976) determined average probe responses when sampling ice crystals and snow. Different average responses were found for different types of crystals and snow. The present study used the average probe response for combined large and small snow (Knollenberg 1975, Fig. 17) to obtain 200Y bin limits as given in Table 1. Presumably a similar correction, though smaller in magnitude, should be applied to measurements from the 2D probes. Since data for any such correction are not available, no adjustment for sizing errors was applied to the 2D data. The general correspondence between spectra from the 2D probes and the 200Y probes, after correction, suggests that any correction for the 2D probes would be much smaller than that used for the 200Y probe. The 2D particles were sized according to their maximum dimension either along the *x*-axis (direction of flight) or along the *y*-axis (array element direction), whichever was larger. Particle concentrations and sample volumes for the 2D probes were adjusted for a 14% clocking error found in the original data (Phillips 1985, personal communication). Particles that shadowed both ends of the array were included. Particles which triggered the probe circuitry, but were too small to be counted, were rejected. Resolution and maximum sizing capability for these probes are given in Table 2.

Particle counts and sample volumes for each of the probes were aggregated into one-minute samples to reduce sampling variations and possible effects of cloud-scale organizations in particle concentrations. Thus,

TABLE 3. Dates and other data relating to snow particle size spectra.

Date	Aircraft Samples			Meteorological Conditions	
	Number	Time interval (EST)	Height above lake (m)	Temperature (°C)	RH (%)
18 Dec 1983	9	1113-1143	88-345	-20 to -17	91-100
19 Dec 1983	15	1027-1301	72-238	-13 to -11	72-100
14 Jan 1984	3	0854-1032	48-369	-8 to -4	91-95
20 Jan 1984	1	1036	374	-24	96
21 Jan 1984	21	1021-1043	52-372	-17 to -14	70-98

each one-minute sample represents an average over about 4.5 km of airplace track. Corresponding sample volumes are about 0.3–0.4 m³ (200Y), 0.1–0.3 m³ (2D-C) and 1–5 m³ (2D-P). Dates, times, flight levels, air temperatures and relative humidities for forty-nine such samples are given in Table 3. Values of relative humidity probably have considerable error because of the slow response of conventional dewpoint hygrometers at the temperatures involved. All data included here were taken within 500 m of the lake surface in regions devoid of liquid drop clouds.

3. Findings and discussion

Figure 1 gives PMS 2D-probe images of snow particles typical of the 49 samples included in this study. Three sections of 2D-C images, and one of 2D-P images, are shown for three different values of ice-water content at three different temperatures. The vertical (array axis) dimension represented in the 2D-C images is about 1.75 mm and that of the 2D-P is about 6.2 mm. The intensity of snowfall is directly related to snow ice water content. Many of the particles in these samples gave quasi-circular 2D-probe images; a small proportion gave quasi-rectangular images. While particles of dendritic habit are regularly observed in lake snows, the dendrite in Fig. 1b is one of the clearer examples found in the 49 samples. The majority of these particles appear to be spatial dendrites and aggregates of dendrites, the arms of which are either too thin to be resolved by the probe, or have evaporated, or both. The degree of riming cannot be reliably estimated because of limited probe resolution, however ground observations (not given here) indicate relatively little riming in lake effect situations as cold as -20°C. Riming was more common at warmer temperatures.

The evidence for aggregation at the colder temperatures is particularly interesting. The coldest sample reported here is from 20 Jan 1984. Figure 2 gives three segments of 2D-C images from that date. This sample was collected at -24°C; the warmest temperature in the sounding was -22°C, about 100 m above the lake; the temperature at cloud top was about -26°C. Upstream, where the particles would have spent part of

their growth time, was even colder. Aggregation is clearly suggested by some of the images in Fig. 2, particularly those marked by small arrows.

At one time it was believed that aggregation was limited to fairly warm temperatures. Our evidence suggests that it can occur at much colder temperatures, at least in lake-effect clouds. Evidence for aggregation at even colder temperatures was presented by Heymsfield (1986).

Figures 3, 4, and 5 show details of size spectra data for the three samples shown in Fig. 1 where the abscissa is the diameter of the snowflake as measured by the probes. These cases were selected as typical of (a) light, (b) moderate, and (c) heavy snow regions (small, medium, and large ice-water content). The degree of correspondence in concentration measured by the different probes depends both on indicated particle size and on snow intensity. Concentrations measured by the 2D-C (dots) were always larger than those from the other two probes, probably because of its superior resolution. The magnitude of this difference ranges from an order of magnitude at the 100–300 μm sizes to a factor of 2 or 3 for 1 mm diam particles. Gordon and Marwitz (1984) also found much higher concentrations in 2D-C probe samples taken at -3.6°C, and slightly higher in samples at -8.8°C, but no difference in samples from colder temperatures.

The curves for the 200Y concentrations (open triangles) tend to flatten out at the smallest sizes. The problem of undersizing and undercounting of ice particles in the first few channels of the 1D-probes has been discussed, and corrections suggested, by Knollenberg (1975), Heymsfield (1976), and Curry and Schemenaur (1979). No adjustments have been applied to data shown here for particle concentrations in the first few channels, [other than the overall size adjustment suggested by Knollenberg (1975)], since subsequent analysis was limited to particles larger than 1 mm.

At sizes larger than about 1 mm, the degree of correspondence in data from the three probes seems to depend upon snow intensity. In the heavier snows (see Fig. 5), the 2D-P concentrations (open circles) often are larger than those from the 200Y. As we go toward moderate snow intensities the data from the two probes gradually merge into a single distribution that char-

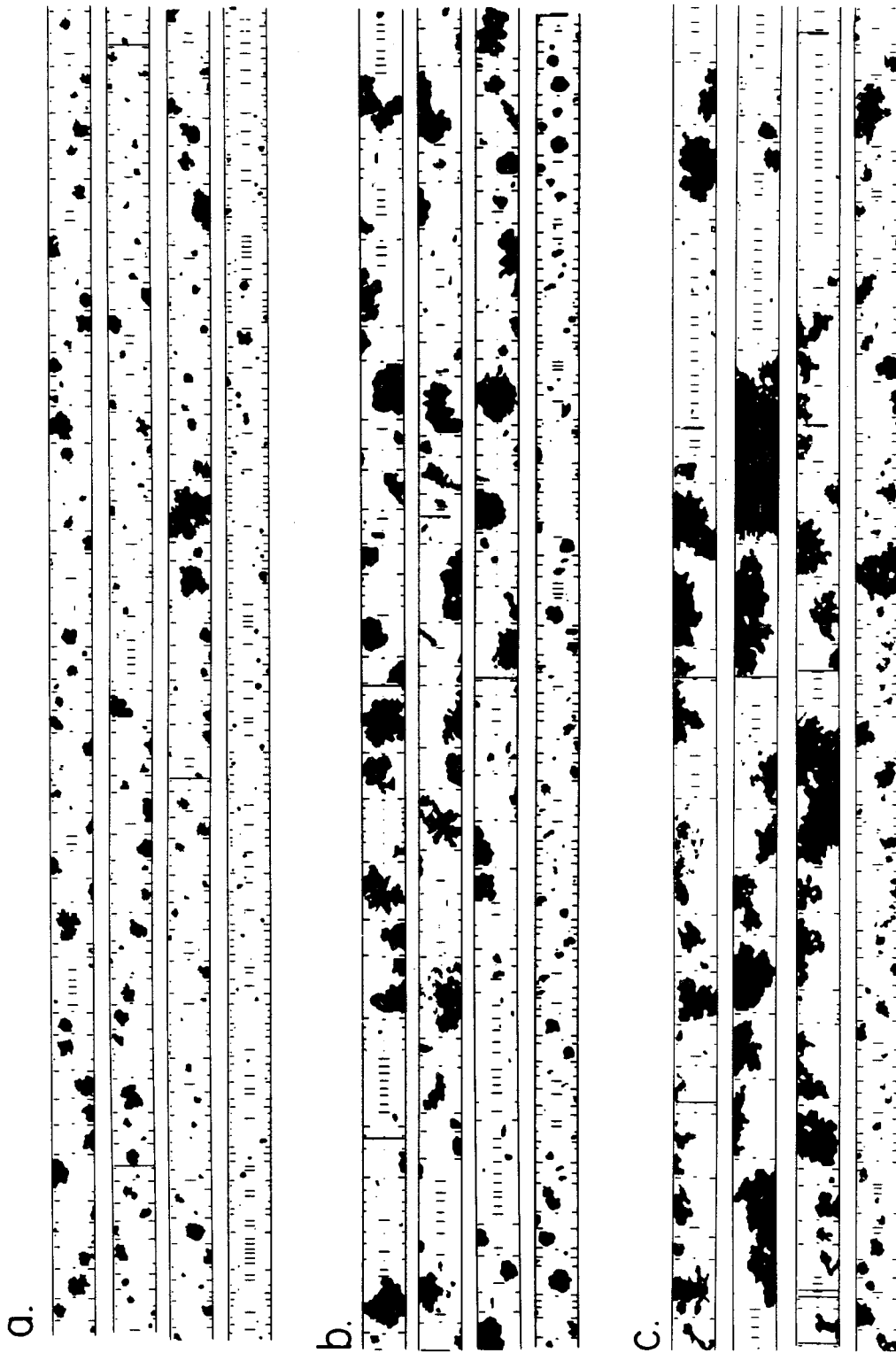


FIG. 1. PMS probe images typical of those involved in this study. Top three panels in each group are from the 2D-C probe. The vertical dimension of these panels corresponds to about 1.75 mm. The bottom panel in each group is from the 2D-P probe; the vertical dimension corresponds to about 6.2 mm. (a) 21 Jan 1984, 1026 EST, IWC 0.005 g m^{-3} , Temp -17°C (b) 14 Jan 1984, 0855 EST, IWC 0.053 g m^{-3} , Temp -4°C (c) 19 Dec 1983, 1301 EST, IWC 0.243 g m^{-3} , Temp -11°C .

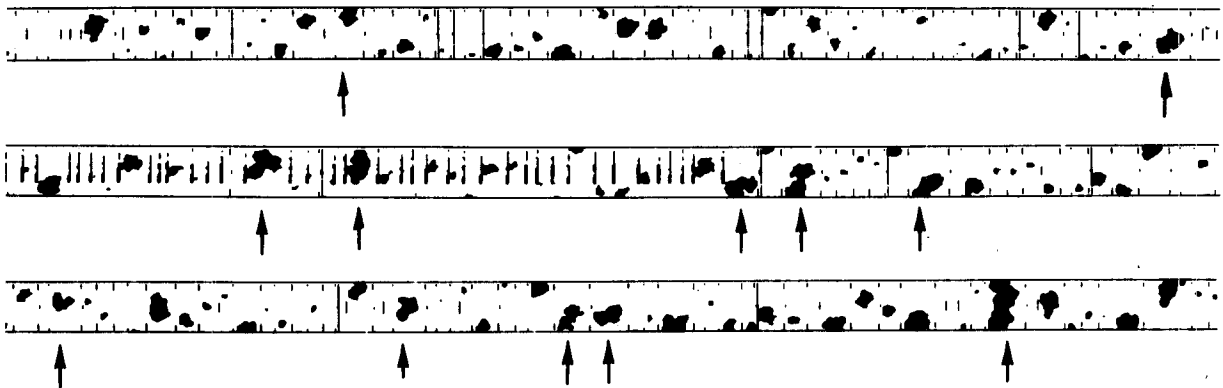


FIG. 2. PMS 2D-C images of snow particles from 1036 EST 20 Jan 1984. Particles showing evidence of aggregation are indicated by arrows. Temperature of collection -24°C .

acterizes both light and moderate snow intensities. The reason for this difference in heavier snows is not known.

Counts in the largest size bin of both the 2D-C and 2D-P are usually well above the trend from smaller size bins. This is to be expected since bin 20 is a "catch-all" bin for particles equal or greater than its threshold size. In our data, bin 19 and bin 20 (two largest sizes) of the 2D-P both are often well above the trend line. Also 2D-P probe bins between 6 and 18 seem to alternately undercount (even-numbered bins) and overcount (odd-numbered bins). Presumably this is a peculiarity of the particular probe.

Consistent with virtually all measurements previously reported, our data indicate an exponential size distribution for snow particles larger than about 1 mm. Exponential distributions were fitted to our measurements of particles larger than 1 mm from all three probes. We used a least squares fit on $\ln N$ vs D and excluded data from bin 20 of the 2D-C and bins 19 and 20 from the 2D-P probes. Table 4 gives parameters of the fitted distributions, $N = N_0 \exp(-\lambda D)$, where N is the concentration of particles per liter per millimeter interval of diameter, N_0 is the zero intercept, λ the slope, D the diameter, and R^2 the coefficient of determination between the data points and the fitted distribution.

The degree to which the fitted distributions characterize the data depends both on particle size and snow intensity. For sizes above about 1 mm the fitted distributions describe the data quite well for moderate snow intensities except for occasional cases where the 2D-P probe gave concentrations well above the 200Y probe values in sizes larger than 4 mm. In the case of light-snow intensities often the best-fitting exponential overestimates concentrations of flakes 2–4 mm diam. This results from the high concentrations reported by the several largest size categories. For the heaviest snow intensities use of both 2D-P and 200Y values often results in a fitted exponential falling between the spectra measured by the two probes. At sizes below about 1 mm, the fitted distributions give concentrations sub-

stantially smaller than those observed by the 2D-C probe. Similar observations were reported by Gordon and Marwitz (1984). For sizes below about 200 μm diameter, the 2D-C concentrations are often an order of magnitude greater than that predicted by our fitted distributions.

From the distribution parameters, total particle concentrations, N_0/λ , were determined. In addition, ice-water content, $\pi N_0/40\lambda^4$, radar reflectivity factor,

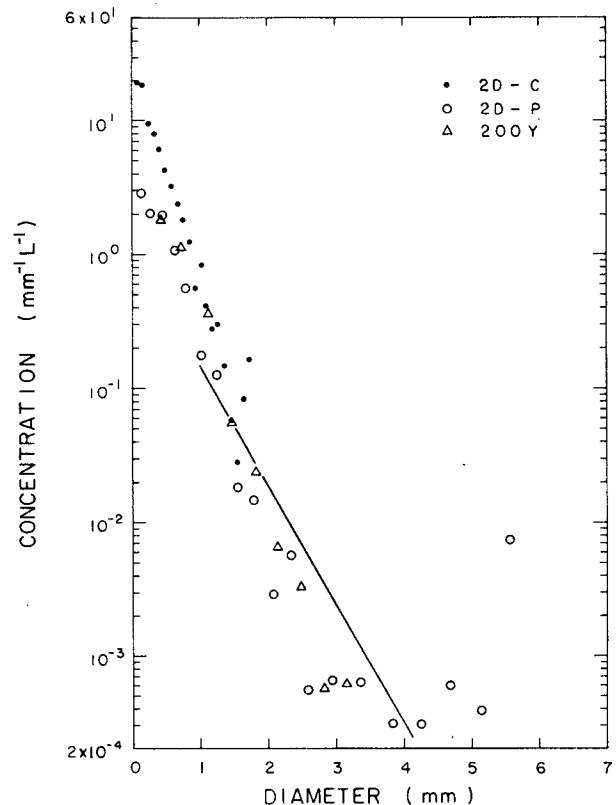


FIG. 3. Snow particle size spectrum typical of light snow; 1026 EST 21 Jan 1984.

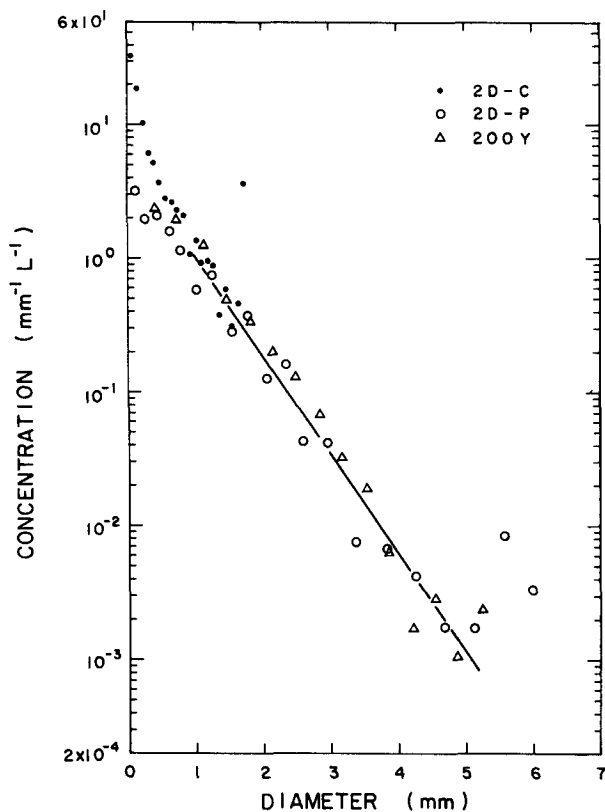


FIG. 4. Same as Fig. 2, except for moderate snow; 0855 EST 14 Jan 1984.

$101N_0/\lambda^7$, and the melted diameter (D_m) of a particle having the mean mass, $0.531/\lambda$, were calculated, using an assumption that these snow particles can be approximated as spheres with bulk density of 0.025 g m^{-3} . The basis for this assumption comes from the studies by Passarelli et al. (1976), Knollenberg (1975) and Magono and Nakamura (1965). Values for these various parameters are given in Table 4, along with detailed data from the 2D-C and 2D-P probes. In Table 4 the samples are ranked in order of increasing ice-water content.

Several interesting trends are evident in Table 4. Ice-water content, obtained by integrating under the exponential size distribution, ranged from about 0.002 to 0.264 g m^{-3} . The value of N_0 increased from less than one to $6.6 \text{ mm}^{-1} \text{ L}^{-1}$, while the slope parameter decreased in going from the smallest to the largest values of ice water content. The total number of particles under the exponential distribution ranged from about 0.4 to more than 5 L^{-1} . We find that total 2D-P concentrations are roughly comparable to those obtained by integrating under the distribution. Concentrations measured by the 2D-C are larger than those obtained by integration by a factor of about 10 at small IWC, decreasing to a factor of about two at large IWC. Cal-

culated radar reflectivity factor ranged from about -6 dBZ to 23 dBZ .

Passarelli et al. (1976), Houze et al. (1979) and Lo and Passarelli (1982) used N_0 - λ trajectories within a snow shaft to infer the dominant snow growth mode. They found that over a broad range of heights, in deep cyclonic snow systems, falling snow growing by aggregation gave trajectories of decreasing N_0 and decreasing λ (slope 1.8 to 1.95), such as indicated by the dashed line in Fig. 6. Different days gave different trajectories, all of about the same slope, but having different values of N_0 . These differences were attributed to different rates of particle initiation and growth in the upper regions where snow growth was dominated by deposition.

As summarized earlier, the growth conditions represented in this study were very different from those of the earlier investigators. Even so, it is informative to compare the N_0 and λ values of the lake-effect snow samples with those reported by the earlier investigators. The envelope in Fig. 6 is a generalized outer limit of data reported by Lo and Passarelli (1982) and Houze et al. (1979).

All but two points fall within the bounds of values presented by Lo and Passarelli (1982) and Houze et al. (1979). We also find a minimum value of λ of about

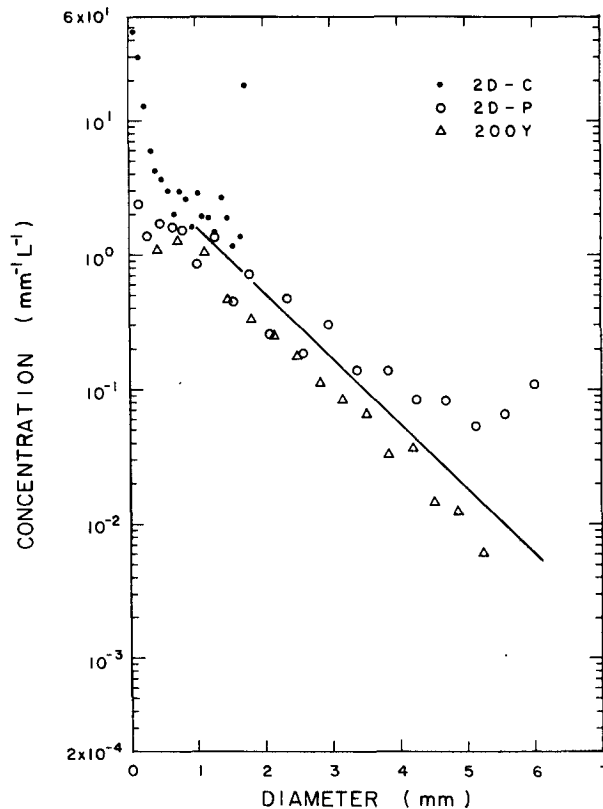


FIG. 5. Same as Fig. 2, except for heavy snow; 1301 EST 19 Dec 1983.

TABLE 4. Distribution parameters and other data for 49 snow spectra.

Date and Time ddMhmm	N_0 $\text{mm}^{-1} \text{L}^{-1}$	λ mm^{-1}	R	Conc. L^{-1}	IWC g m^{-3}	Z_e dBz	D_m mm	2D-C			2D-P		
								Volume L	Particle Counts	Conc. L^{-1}	Volume L	Particle Counts	Conc. L^{-1}
21J1025	1.18	2.42	0.86	0.49	0.003	-6.10	0.022	243.4	786	3.23	3519.6	3074	0.87
21J1041	0.72	2.00	0.90	0.36	0.004	-2.44	0.027	336.6	999	2.97	6051.8	3760	0.62
21J1024	0.75	1.99	0.86	0.38	0.004	-2.15	0.027	280.6	1166	4.16	4205.1	4068	0.97
21J1029	0.97	1.88	0.89	0.52	0.006	0.72	0.028	186.6	1200	6.43	5341.5	4093	0.77
21J1026	1.34	2.01	0.88	0.67	0.006	0.07	0.026	258.3	1724	6.67	4993.3	7896	1.58
21J1030	2.00	2.20	0.95	0.91	0.007	-0.91	0.024	225.2	1369	6.08	4548.1	5694	1.25
21J1034	1.11	1.89	0.91	0.59	0.007	1.15	0.028	372.5	1515	4.07	4574.2	5846	0.99
21J1043	1.68	2.08	0.94	0.81	0.007	0.03	0.026	267.8	1236	4.62	5383.0	3754	0.70
20J1036	0.42	1.47	0.82	0.29	0.007	4.56	0.036	207.7	2503	12.05	3063.9	6536	2.13
21J1038	2.79	2.34	0.96	1.19	0.007	-1.36	0.023	297.3	1798	6.05	5564.0	7289	1.31
19D1135	1.04	1.79	0.96	0.58	0.008	2.49	0.030	370.4	1058	2.86	5447.6	3147	0.58
18D1123	1.94	2.02	0.91	0.96	0.009	1.54	0.026	373.8	1866	4.99	5201.1	5777	1.11
18D1143	3.84	2.36	0.95	1.63	0.010	-0.25	0.022	518.5	2257	4.35	4574.5	5255	1.15
21J1022	1.94	1.97	0.93	0.98	0.010	2.30	0.027	179.4	1394	7.77	4947.8	4956	1.00
21J1035	2.70	2.14	0.93	1.26	0.010	1.23	0.025	337.0	1593	4.73	5250.5	4882	0.93
21J1039	2.38	2.03	0.96	1.17	0.011	2.27	0.026	330.4	1828	5.53	5801.0	7261	1.25
21J1021	1.89	1.85	0.93	1.02	0.013	4.11	0.029	286.8	1809	6.31	3531.8	6711	1.90
21J1042	2.19	1.89	0.96	1.16	0.013	4.08	0.028	323.4	1510	4.67	4629.7	4497	0.97
21J1023	3.81	2.14	0.89	1.78	0.014	2.71	0.025	214.2	2120	9.90	4374.4	6449	1.47
18D1114	4.35	2.17	0.94	2.00	0.015	2.87	0.024	195.1	1698	8.70	5484.8	6941	1.27
18D1116	5.65	2.25	0.94	2.51	0.017	2.90	0.024	296.0	2584	8.73	3514.3	5950	1.69
21J1040	2.87	1.84	0.95	1.56	0.020	6.08	0.029	261.8	1649	6.30	4659.6	5749	1.23
18D1137	5.80	2.18	0.94	2.66	0.020	3.98	0.024	375.4	2522	6.72	3440.0	5801	1.69
21J1031	3.36	1.90	0.97	1.77	0.020	5.78	0.028	275.3	1951	7.09	4130.8	6110	1.48
18D1127	5.49	2.08	0.93	2.64	0.023	5.17	0.026	294.1	2743	9.33	3219.5	4905	1.52
21J1028	5.10	2.03	0.91	2.51	0.024	5.59	0.026	241.6	2464	10.20	3221.7	6275	1.95
18D1126	4.81	1.97	0.93	2.44	0.025	6.24	0.027	246.0	2087	8.48	3270.3	5864	1.79
18D1113	7.90	2.21	0.95	3.57	0.026	4.90	0.024	273.9	2577	9.41	3025.8	4935	1.63
18D1141	6.14	2.04	0.92	3.01	0.028	6.24	0.026	223.9	2065	9.22	2403.7	6655	2.77
21J1033	2.90	1.68	0.97	1.72	0.029	8.88	0.032	224.2	1289	5.75	4308.1	6224	1.44
14J1032	0.40	1.01	0.90	0.40	0.030	15.86	0.053	342.6	647	1.89	6902.2	2020	0.29
21J1027	5.20	1.86	0.95	2.80	0.034	8.33	0.028	220.7	2363	10.71	2481.9	6962	2.81
19D1134	4.89	1.65	0.96	2.96	0.052	11.70	0.032	180.3	628	3.48	2555.5	6646	2.60
14J0855	8.15	1.77	0.98	4.60	0.065	11.79	0.030	141.3	1155	8.17	2547.3	6094	2.39
19D1043	3.97	1.42	0.93	2.79	0.077	15.36	0.037	165.2	1453	8.80	2411.8	5906	2.45
19D1027	5.88	1.50	0.94	3.92	0.091	15.40	0.035	167.5	1385	8.27	2313.0	6105	2.64
21J1032	7.23	1.56	0.97	4.64	0.096	15.11	0.034	171.8	1685	9.81	3455.2	7106	2.06
19D1040	2.97	1.23	0.93	2.41	0.102	18.47	0.043	158.5	1402	8.85	1675.2	3103	1.85
19D1042	6.20	1.47	0.96	4.22	0.104	16.24	0.036	215.4	2298	10.67	1224.2	3760	3.07
14J0854	6.46	1.48	0.98	4.37	0.106	16.22	0.036	156.5	1130	7.22	2625.5	5117	1.95
19D1132	2.54	1.17	0.96	2.17	0.106	19.30	0.045	177.3	1471	8.30	2517.9	5553	2.21
19D1030	7.19	1.48	0.88	4.86	0.118	16.68	0.036	138.7	1127	8.13	2468.3	4666	1.89
19D1028	5.14	1.30	0.92	3.95	0.141	19.17	0.041	96.4	942	9.77	2116.0	4958	2.34
19D1133	8.04	1.39	0.94	5.78	0.169	19.08	0.038	99.9	1257	12.58	1613.0	5529	3.43
19D1217	7.10	1.34	0.93	5.30	0.173	19.65	0.040	106.1	1349	12.71	1666.1	5518	3.31
19D1029	5.87	1.23	0.92	4.78	0.202	21.43	0.043	91.4	990	10.83	1666.7	4659	2.80
19D1041	6.40	1.23	0.93	5.20	0.220	21.80	0.043	132.9	1607	12.09	951.1	2985	3.14
19D1301	6.40	1.14	0.90	5.61	0.298	24.11	0.047	62.5	846	13.54	1241.9	4367	3.52
19D1057	8.75	1.21	0.92	7.23	0.321	23.66	0.044	57.7	920	15.94	1088.3	4811	4.42

10 cm^{-1} even though our data came from a very different type of meteorological situation. Passarelli attributed the lower bound in λ as due to the onset of particle breakup, though why it corresponded to 10 cm^{-1} was not known. As seen in Fig. 6, our data give values of λ ranging from about 10 to 24 cm^{-1} . If the minimum value of λ is related to the onset of breakup of snowflakes, as suggested by Lo and Passarelli (1982), the larger values found in these data may indicate enhanced turbulence at low levels in the convective boundary layer accompanying lake-effect snows.

4. Conclusions

In situ snow particle sizes and concentrations were measured at low levels over Lake Michigan during lake-

effect snow storms. Forty-nine samples reported here are consistent with, and extend, the limited data previously published on in situ snow spectra.

The particles appear to be predominantly spatial dendrites and aggregates of dendritic forms, but limited resolution of the PMS probes for snow particles obscure details of crystal structures. Aggregation at a temperature of -24°C is clearly indicated.

Data from PMS 200Y, 2D-C and 2D-P probes showed general agreement for sizes larger than about 1 mm diam. For sizes below about 1 mm the 2D-C probe provide the best data because of its superior resolution. At these small sizes, concentrations indicated by the 2D-C are substantially above those indicated by an exponential fitted to sizes above 1 mm diam.

Exponential distributions fitted to data for sizes

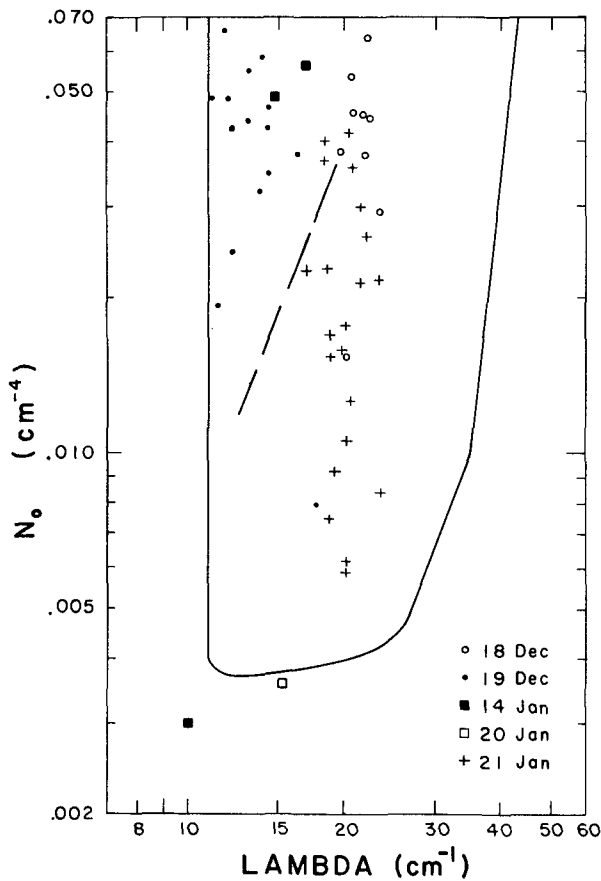


FIG. 6. Snow size-distribution parameters for 49 samples. Dashed line gives the slope of aggregation trajectories as deduced by Lo and Passarelli (1982) and others; see text.

larger than 1 mm were used to calculate several distribution parameters. Particle concentrations implied by the exponential distribution ranged from 0.36 to 5.85 L^{-1} ; ice-water contents ranged from about 0.002 to 0.264 $g\ m^{-3}$. Slope and intercept values of these distributions fall within the range of values previously reported. These data are consistent with the work of Lo and Passarelli (1982) who found a value of 10 cm^{-1} for the lower bound of the slope parameter (λ).

Acknowledgments. Measurements used in this study were obtained under National Science Foundation Grant ATM 83-10429. The instrumented airplane was provided and operated by the National Center for Atmospheric Research, operating under support from the National Science Foundation. We are grateful to NCAR ATD scientists for installation and calibration of the PMS Particle Probes.

Data analysis was supported under NSF Grant ATM 86-17177. The assistance of Maureen Dungey for data

reduction and preparation of the manuscript and to anonymous reviewers for helpful suggestions is gratefully acknowledged.

REFERENCES

- Battan, L. J., 1973: *Radar Observation of the Atmosphere*. University of Chicago Press, 324 pp.
- Curry, M. J., and R. S. Schemenaur, 1979: The small-particle response of an optical array precipitation probe. *J. Appl. Meteor.*, **18**, 816-821.
- Gordon, G. L., and J. D. Marwitz, 1984: An airborne comparison of three PMS Probes. *J. Atmos. Oceanic Technol.*, **1**, 22-27.
- Gunn, K. L. S., and J. S. Marshall, 1958: The distribution with size of aggregate snowflakes. *J. Meteor.*, **15**, 452-461.
- Heymsfield, A. J., 1976: Particle size distribution measurement: An evaluation of the Knollenberg optical array probes. *Atmos. Technol.*, **8**, National Center for Atmospheric Research, 17-24.
- , 1986: Ice particle evolution in the anvil of a severe thunderstorm during CCOPE. *J. Atmos. Sci.*, **43**, 2463-2478.
- Houze, R. A., Jr., P. V. Hobbs, P. H. Herzegh and D. B. Parsons, 1979: Size distributions of precipitation particles in frontal clouds. *J. Atmos. Sci.*, **36**, 156-162.
- Knollenberg, R. G., 1970: The optical array: An alternative to scattering or extinction for airborne particle size determination. *J. Appl. Meteor.*, **9**, 86-103.
- , 1975: The response of optical array spectrometers to ice and snow: A study of probe size to crystal mass relationships. Air Force Cambridge Res. Lab. Rep. AFCRL-TR-75-0494, 70 pp.
- , 1976: Response of optical array spectrometers to ice and snow: A study of 2D-probe area-to-mass relationships. Air Force Cambridge Res. Lab. Rep. TR-76-0273, 31 pp.
- , 1981: Techniques for probing cloud microstructure. *Clouds: Their Formation, Optical Properties, and Effects*. P. V. Hobbs and A. Deepak, Eds., Academic Press, 15-92.
- Lo, K. H., and R. E. Passarelli, Jr., 1982: The growth of snow in winter storms: An airborne observational study. *J. Atmos. Sci.*, **39**, 697-706.
- Magono, C., and T. Nakamura, 1965: Aerodynamic studies of falling snowflakes. *J. Meteor. Soc. Japan*, **43**(3), 139-147.
- Marshall, J. S., and K. L. S. Gunn, 1952: Measurement of snow parameters by radar. *J. Meteor.*, **15**, 452-466.
- Ohtake, T., 1965: Preliminary observations on size distribution of snowflakes and raindrops at just above and below the melting layer. *Proc. Int'l. Conf. on Cloud Physics*, Tokyo and Sapporo. Int. Assn. Meteor. Atmos. Phys., 271-275.
- , 1968: Changes in size distribution of hydrometeors through a melting layer. *Proc. Thirteenth Conf. on Radar Meteor.*, Montreal. Amer. Meteor. Soc., Boston, 148-153.
- Passarelli, R. E., Jr., 1978a: *The evolution of snow size spectra in winter storms*. Ph.D. thesis, The University of Chicago, 100 pp.
- , 1978b: An analytical model of snowflake growth. Preprints, *Conf. on Cloud Physics and Atmospheric Electricity*, Issaquah. Amer. Meteor. Soc., Boston, 142-147.
- , N. J. Carrera and R. R. Braham, Jr., 1976: Comparison of radar and aircraft measurements of snow size spectra in a Midwest winter snowstorm. Preprints, *Seventeenth Conf. on Radar Meteorology*, Seattle. Amer. Meteor. Soc., Boston, 214-219.
- Rogers, D. C., 1974: An observational study of aggregation. *Proc., Conf. on Cloud Physics*, Tucson. Amer. Meteor. Soc., Boston, 108-111.
- Sekhon, R. S., and R. Srivastava, 1970: Snow size spectra and radar reflectivity. *J. Atmos. Sci.*, **27**, 299-307.
- Smith, P. L., 1984: Equivalent radar reflectivity factors for snow and ice particles. *J. Climate Appl. Meteor.*, **23**, 1258-1260.